*fermentation*

MDPI

*Article*

# Development of Volatile Fatty Acid and Methane Production Prediction Model Using Ruminant Nutrition Comparison of Algorithms

**Myungsun Park [1,2], Sangbuem Cho [2], Eunjeong Jeon [2,3] and Nag-Jin Choi [2,*]**

[1] Hanwoo Research Institute, National Institute of Animal Science, Pyeongchang 25340, Republic of Korea; sunnypark411@korea.kr
[2] Department of Animal Science, Jeonbuk National University, Jeonju 54896, Republic of Korea
[3] Department of Animal Science, College of Agriculture and Natural Resources, Michigan State University, East Lansing, MI 48824, USA
* Correspondence: nagjin@jbnu.ac.kr; Tel.: +82-63-270-2579; Fax: +82-63-270-2612

**Abstract:** (1) Background: This study explores the correlation between volatile fatty acid (VFA) concentrations and methanogenesis in ruminants, focusing on how the nutritional composition of their diets affects these processes. (2) Methods: We developed predictive models using multiple linear regression, artificial neural networks, and *k*-nearest neighbor algorithms. The models are based on data extracted from 31 research papers and 16 ruminal in vitro fermentation tests to predict VFA concentrations from nutrient intake. Methane production estimates were derived by converting and clustering these predicted VFA values into molar ratios. (3) Results: This study found that acetate concentrations correlate significantly with neutral detergent fiber intake. Conversely, propionate and butyrate concentrations are highly dependent on dry matter intake. There was a notable correlation between methane production and the concentrations of acetate and butyrate. Increases in neutral detergent fiber intake were associated with higher levels of acetate, butyrate, and methane production. Among the three methods, the k-nearest neighbor algorithm performed best in terms of statistical fitting. (4) Conclusions: It is vital to determine the optimal intake levels of neutral detergent fiber to minimize methane emissions and reduce energy loss in ruminants. The predictive accuracy of VFA and methane models can be enhanced through experimental data collected from diverse environmental conditions, which will aid in determining optimal VFA and methane levels.

**Keywords:** methane production; nutrient intake; ruminant metabolism; volatile fatty acid

check for updates

**Citation:** Park, M.; Cho, S.; Jeon, E.; Choi, N.-J. Development of Volatile Fatty Acid and Methane Production Prediction Model Using Ruminant Nutrition Comparison of Algorithms. *Fermentation* **2024**, *10*, 410. https://doi.org/10.3390/fermentation10080410

Academic Editors: Guijie Chen, Zhuqing Dai and Chunxu Chen

Received: 21 May 2024
Revised: 5 August 2024
Accepted: 7 August 2024
Published: 8 August 2024

**Copyright:** © 2024 by the authors. Licensee MDPI, Basel, Switzerland. This article is an open access article distributed under the terms and conditions of the Creative Commons Attribution (CC BY) license (https://creativecommons.org/licenses/by/4.0/).

## 1. Introduction

Ruminant feed is categorized into two main types: coarse forage, composed of structured carbohydrates, and an enriched concentrate containing non-structured carbohydrates. Carbohydrates, ingested as feed, undergo microbial decomposition in the rumen, giving rise to volatile fatty acids (VFAs). VFAs represent crucial metabolites, contributing up to 75% of the total metabolic energy of ruminants [1,2]. Among VFAs, acetate (C2) constitutes around 70%, propionate (C3) 20%, and butyrate (C4) 10% [3]. These percentages are on a molar basis. The proportion of C2 derived from pyruvate escalates with increasing forage consumption [4,5]. Propionate levels, which also rise with increased feed intake, play a pivotal role in body fat formation [6,7]. Additionally, propionate, which plays a significant role in methane production, is also a major contributor to gluconeogenesis. Butyrate, typically produced during acetate–lactate fermentation by Clostridium butyricum, is associated with the development of rumen papilla [8,9]. The VFAs exhibit a close relationship with hydrogen dynamics, where C3 utilizes hydrogen, and C2 produces hydrogen [10,11]. Most of the hydrogen generated in this process is eventually converted into methane by

methanogens. Methane is primarily produced by hydrogenotrophic methanogens using hydrogen as a substrate, while the contribution of acetoclastic methanogenesis, which utilizes acetic acid, is relatively minor. This methane production leads to an energy loss of 2–12% in ruminants [12,13]. Reducing methane production is urgent due to its 21-times-higher global warming potential than carbon dioxide [14]. Methane production varies based on VFA composition, and ruminal VFAs change according to feed intake and feed nutrient composition. Therefore, accurate prediction of VFAs and methane levels resulting from feed intake is crucial for both global environmental sustainability and farm productivity.

Several studies have employed multiple linear regression (MLR) to predict rumen VFA concentrations using feed nutrients as independent variables [15–17]. In addition, some studies have used VFA concentrations in the rumen to predict methane production [18–21]. Although MLR exhibits excellent predictive accuracy in linear data structures, its accuracy diminishes with complex interrelationships. Artificial neural networks (ANNs) have proven valuable in studying the complex process of rumen fermentation, demonstrating high accuracy in predicting rumen fermentation patterns [22,23]. Li et al. [24] reported superior model performance indicators, such as $R^2$ (R-squared) for ANN compared to MLR in predicting VFA, albeit without significant accuracy improvement. Previous studies have highlighted the efficacy of the *k*-nearest neighbor (KNN) algorithm, a nonparametric method, in predicting volatile fatty acids from nutritional components and methane from volatile fatty acid content in complex, nonlinear data structures [25].

This study utilizes three distinct predictive algorithms (MLR, ANN, KNN) to forecast volatile fatty acid (VFA) levels based on nutrient intake, as well as methane production from rumen metabolites. The primary goal is to evaluate the impact of feed nutrient intake on VFA production and methanogenesis within the rumen. All models developed in this research leverage these algorithms, and their predictive accuracies are compared to identify the most suitable model for predicting VFAs and methane levels. Additionally, this study predicts VFAs in the rumen using feed nutrient intake data and then utilizes these predicted VFAs to estimate methane production. This methodology aims to provide a practical solution for overcoming the challenges of measuring gaseous methane directly on farms, by offering a way to predict farm-specific methane emissions based on feed intake levels. This approach intends to support farm management in optimizing feeding strategies and mitigating methane emissions effectively.

## 2. Materials and Methods

### *2.1. Data Collection and Descriptive Statistics*

Descriptive statistics for the data collected from 31 articles are presented in Table 1, including 16 in vitro experiments conducted in a laboratory (Table 2). Volatile fatty acid concentrations were predicted based on the intake of dry matter (DM), crude protein (CP), ether extract (EE), organic matter (OM), neutral detergent fiber (NDF), acid detergent insoluble fiber (ADF), and total digestible nutrients (TDN).

**Table 1.** Summary of means of the data used for predicting volatile fatty acid concentrations and methane production.

| Study * | Animal | Type | N | DMI | C2 | C3 | C4 | TVFA | $CH_4$ |
|---|---|---|---|---|---|---|---|---|---|
| Ahn et al. [26] | Beef | vit | - | - | 26.64 | 19.41 | 11.60 | 57.66 | - |
| Beauchemin et al. [27] | Beef | vivo | 4 | 8.61 | 52.68 | 34.03 | 9.43 | 97.53 | 110.70 |
| Beauchemin et al. [28] | Beef | vivo | 4 | 6.42 | 53.86 | 18.66 | 8.53 | 85.05 | 150.25 |
| Beauchemin et al. [29] | Beef | vivo | 3 | 5.69 | 65.27 | 19.20 | 10.50 | 103.17 | 99.17 |
| Beauchemin et al. [30] | Dairy | vivo | 4 | 19.33 | 60.45 | 25.93 | 9.14 | 110.50 | 265.75 |
| Benchaar et al. [31] | Dairy | vivo | 4 | 24.45 | 62.00 | 22.33 | 12.50 | 95.03 | 484.25 |
| Biswas et al. [32] | Beef | vivo, vit | 5 | 6.04 | 35.12 | 16.71 | 17.61 | 69.43 | - |
| Bougouin et al. [33] | Dairy | vivo | 4 | 22.80 | 37.96 | 8.96 | 5.60 | 54.20 | 438.50 |
| Bougouin et al. [34] | Dairy | vivo | 4 | 18.50 | 38.66 | 11.31 | 6.70 | 59.10 | 355.78 |

**Table 1.** *Cont.*

| Study * | Animal | Type | N | DMI | C2 | C3 | C4 | TVFA | $CH_4$ |
|---|---|---|---|---|---|---|---|---|---|
| Guyader et al. [35] | Dairy | vit | 2 | - | 70.40 | 16.13 | 9.84 | 90.66 | 251.55 |
| Hassanat et al. [36] | Dairy | vivo | 3 | 23.60 | 67.23 | 19.33 | 10.67 | 98.11 | 483.33 |
| Hatew et al. [37] | Dairy | vivo | 4 | 18.98 | 68.48 | 16.13 | 11.40 | 99.96 | 415.25 |
| Holtshausen et al. [38] | Dairy | vit | 3 | - | 58.67 | 23.20 | 13.56 | 140.65 | 377.90 |
| Jeon et al. [39] | Beef | vivo, vit | 24 | 7.35 | 48.50 | 15.19 | 11.10 | 75.08 | - |
| Jeong et al. [40] | Beef | vit | - | - | 35.54 | 15.84 | 11.76 | 64.69 | - |
| Kim et al. [41] | Beef | vit | - | - | 48.34 | 39.44 | 7.34 | 95.13 | - |
| Kim et al. [42] | Beef | vit | - | - | 56.74 | 28.18 | 12.93 | 102.23 | - |
| Kim et al. [43] | Beef | vit | - | - | 61.04 | 27.66 | 23.52 | 118.05 | - |
| Kim et al. [44] | Beef | vivo, vit | 5 | 6.03 | 23.45 | 14.46 | 15.47 | 53.37 | - |
| Kook et al. [45] | Beef | vivo, vit | 45 | 6.89 | 68.37 | 26.75 | 17.26 | 122.30 | - |
| Lee et al. [46] | Beef | vit | - | - | 37.83 | 14.951 | 7.9 | 64.06 | - |
| Lee et al. [47] | Beef | vivo, vit | 4 | 8.43 | 32.87 | 10.64 | 5.26 | 51.20 | - |
| Mamuad et al. [48] | Beef | vivo, vit | 27 | 9.35 | 41.98 | 16.81 | 13.48 | 72.27 | - |
| Miguel et al. [49] | Beef | vit | - | - | 55.32 | 18.98 | 13.00 | 87.29 | - |
| Moate et al. [50] | Dairy | vivo | 32 | 22.15 | 64.43 | 25.24 | 10.56 | 104.25 | 449.25 |
| Nogoy et al. [51] | Beef | vivo, situ | 2 | 5.63 | 37.47 | 14.74 | 2.52 | 60.68 | - |
| Park et al. [52] | Beef | vit | - | - | 13.29 | 8.92 | 2.23 | 58.58 | - |
| van Zijderveid et al. [53] | Dairy | vit | - | 19.90 | 77.68 | 27.88 | 18.91 | 130.6 | 343.50 |
| Yang et al. [54] | Beef | vit, situ | 2 | - | 25.30 | 14.58 | 5.15 | 47.53 | - |
| Yang et al. [55] | Beef | vit | - | - | 49.23 | 20.48 | 12.82 | 87.15 | - |
| Yoo et al. [56] | Beef | vit | - | - | 44.84 | 16.22 | 10.71 | 80.71 | - |

* vit, rumen in vitro fermentation experiments; vivo, rumen in vivo fermentation experiments; situ, in situ experiments; N, number of animals; DMI, dry matter intake (kg/d); C2, acetate (mM); C3, propionate (mM); C4, butyrate (mM); TVFA, total volatile fatty acid (mM); $CH_4$, methane (g/d).

**Table 2.** Nutrient intake and ruminal production data used for predictive modeling.

| Item [1] | N | Mean | SD [2] | Minimum | Median | Maximum |
|---|---|---|---|---|---|---|
| Nutrient intake (kg/d) | | | | | | |
| DM | 98 | 14.34 | 6.20 | 5.63 | 13.65 | 25.20 |
| CP | 71 | 2.06 | 1.22 | 0.68 | 1.29 | 4.23 |
| EE | 8 | 0.57 | 0.47 | 0.23 | 0.28 | 1.22 |
| OM | 24 | 11.97 | 6.66 | 5.63 | 6.81 | 21.44 |
| NDF | 68 | 5.11 | 2.39 | 1.08 | 4.09 | 9.81 |
| ADF | 68 | 2.97 | 1.61 | 0.30 | 2.38 | 5.87 |
| Diet composition (% of DM) | | | | | | |
| CP | 219 | 13.12 | 4.45 | 1.44 | 14.50 | 19.58 |
| EE | 160 | 2.52 | 1.32 | 0.46 | 2.31 | 7.16 |
| OM | 176 | 94.01 | 3.22 | 86.11 | 94.20 | 98.88 |
| NDF | 211 | 36.88 | 16.97 | 2.70 | 1.70 | 70.88 |
| ADF | 205 | 22.10 | 11.82 | 1.70 | 22.48 | 49.83 |
| TDN | 23 | 73.88 | 6.93 | 54.80 | 71.45 | 88.00 |
| Ruminal production (mM) | | | | | | |
| C2 | 251 | 50.57 | 15.12 | 12.61 | 52.40 | 81.35 |
| C3 | 251 | 19.24 | 6.60 | 5.14 | 17.98 | 45.70 |
| C4 | 251 | 9.56 | 5.38 | 0.39 | 10.10 | 34.44 |
| TVFA | 251 | 85.15 | 24.85 | 24.74 | 87.39 | 156.52 |
| Methane (g/d) | 88 | 304.86 | 151.09 | 62.10 | 419.35 | 635.00 |

[1] DM, dry matter; CP, crude protein; EE, ether extract; OM, organic matter; NDF, neutral detergent fiber; ADF, acid detergent fiber; TDN, total digestible nutrients; C2, acetate; C3, propionate; C4, butyrate; TVFA, total volatile fatty acid. [2] N, number of data; SD, standard deviation.

In vitro fermentation data were analyzed by combining the results from the papers and laboratory experiments conducted over 24 h. Additionally, VFAs were presented as molar ratios to align with the in vivo data.

### *2.2. In Vitro Batch Fermentation*

Two non-lactating dairy cows with rumen cannulas were donors for ruminal inoculum. Feed was provided at specific intervals (8:00 a.m. and 5:00 p.m.). Ruminal fluid collected before morning feeding was mixed, filtered through cheesecloth, placed in an insulated bottle at 39 °C and transferred to the laboratory. This fluid was mixed with McDougall's buffer [57] and artificial saliva (1:4 $v/v$ ratio). Afterward, 50 mL of this buffered rumen fluid was dispensed into individual 250 mL serum bottles containing pre-weighed 0.5 g substrate and additive. Experiments were conducted in triplicate (n = 3) using a fully randomized experimental design. Serum bottles were sealed to maintain anaerobicity, and carbon dioxide ($CO_2$) gas was dispensed to ensure anaerobic conditions. Gas production was monitored after 24 h of incubation at 39 °C.

### *2.3. Measurement of Rumen Fermentation Parameters*

Quantifying the outcome of our experiments involved a multi-faceted approach. The total gas produced was meticulously measured using 100 milliliter (mL) calibrated glass syringes attached to a 20-gauge, 30.5 cm needle (Popper®, Fisher Scientific, Hampton, NH, USA). For in vitro experiments, gases were collected using aluminum packs with rubber inserts. Subsequent analysis involved using the gases collected in these aluminum gas packs. We adopted the method proposed by Lopez et al. [58] with slight modifications for the quantification of $CH_4$ and $H_2$. Gas chromatography (HP7890, Agilent Technologies, Santa Clara, CA, USA), equipped with a thermal conductivity detector and a capillary column, was utilized for this purpose. The VFA analysis, another integral aspect of our study, involved stabilizing samples with the addition of 0.2 mL of 25% ($w/v$) metaphosphoric acid (Sigma-Aldrich, St. Louis, MO, USA), followed by analysis using gas chromatography [59]. Furthermore, ammonia-N was determined according to Chaney and Marbach [60].

### *2.4. Development of the Prediction Models*

The data were normalized using the following equation before developing the prediction models:

$$x_{norm} = \frac{x - x_{min}}{x_{max} - x_{min}} \quad (1)$$

In Equation (1), $x_{norm}$ is the normalized data set, x is the observed data set, $x_{min}$ is the minimum value of the data set, and $x_{max}$ is the maximum value of the data set. The MLR equation used for the dependent variable $Y$ and independent variable groups $x$ and β is as follows:

$$Y = \beta_0 + \beta_1 x_1 + \beta_2 x_2 \cdots \beta_n x_n + \varepsilon \quad (2)$$

In Equation (2), $\beta$ represents the linear regression coefficients, and $\varepsilon$ represents the error. After developing the model, the data were denormalized using the following equation to match the units of the predicted and observed values:

$$x_{denorm} = x_{norm}(x_{max} - x_{min}) + x_{min} \quad (3)$$

In Equation (3), $x_{denorm}$ is the denormalized data and $x_{norm}$, $x_{min}$, and $x_{max}$ are as defined before. To predict dry matter intake in the rumen in vitro experiment, independent variables were designated as C2, C3, C4, and total volatile fatty acid. Residual nutrient intake was calculated based on predicted DMI and played a crucial role in forecasting volatile fatty acid concentrations. A volatile fatty acid prediction model was developed to anticipate the produced amounts of acetate (MC2, mol/100 mol), propionate (MC3, mol/100 mol), butyrate (MC4, mol/100 mol), and TVFAs (mM) using feed nutrient intake as an independent variable. In addition, C2, C3, and C4 were calculated using TVFA, and

then the predicted and observed values were visualized and compared. To construct a methane prediction model, MC2, MC3, MC4, and TVFA were clustered using the *K*-means (KM) clustering algorithm:

$$J = \sum_{j=1}^{k} \sum_{i=1}^{n} \left\| x_i^j - c_j \right\|^2 \quad (4)$$

In Equation (4), $J$ is the objective function, $k$ is the number of clusters, $n$ is the number of cases, $x_i$ is the case $i$, and $c_j$ is the centroid for cluster $j$. Initial clustering of volatile fatty acids was performed using the *K*-means clustering algorithm, with the number of clusters determined by the elbow criterion, dependent on the data type. A predictive model for methanogenesis was then developed using the clustered volatile fatty acids as independent variables. The significance of each regression coefficient was verified using the ordinary least squares method (OLS) to verify the prediction models.

$$y = \frac{1}{k} \sum_{j=1}^{k} y_{ij} \quad (5)$$

In Equation (5), $y$ is the prediction of *k*-nearest neighbor, $k$ is select k closest instances, $i$ is the independent variable, and $j$ is the dependent variable. In this study, $k$ values were set from 1 to 10 and analyzed, and all KNN models were developed using the $k$ value with the smallest root mean squared error (RMSE):

$$\mathrm{RMSE} = \sqrt{\frac{1}{n} \sum_{i=1}^{n} (y_i - \hat{y}_i)^2} \quad (6)$$

In Equation (6), n represents the number of observations, $\hat{y}_i$ is the observed value for the $i$th observation, and $\hat{y}_i$ is the predicted value for the $i$th observation. All models based on the ANN algorithm used the Rectified Linear Unit (ReLu) as the activation function:

$$z = f(\sum_{i=1}^{n} x_i \omega_i) \quad (7)$$

In Equation (7), $z$ represents the prediction of the ANN model, $f$ is the activation function, $x$ represents input data, $w$ represents weights, and n represents the number of input layers. The ANN model was developed with three hidden layers. Additionally, the *k*-nearest neighbor equations used for the DMI, VFA, and methane prediction models were different, and the ANN made predictions in the same manner as the MLR algorithm.

### *2.5. Statistics Analysis*

Each prediction model was validated when development confirmed the prediction accuracy by obtaining the RMSE and $R^2$ (coefficient of determination):

$$R^2 = 1 - \frac{\sum (y_i - \hat{y})^2}{\sum (y_i - \overline{y})^2} \quad (8)$$

where $n$ is the number of observations, $y_i$ is the observed value for the $i$th observation, $\hat{y}$ is the predicted value, and $\overline{y}$ is the mean value of $y$. The MAE (mean absolute error) of the measured and predicted values was calculated as follows:

$$\mathrm{MAE} = \frac{1}{n} \sum_{i=1}^{n} |y_i - \hat{y}| \quad (9)$$

where $n$ is the number of observations, $y_i$ is the observed value for the $i$th observation, and $\hat{y}$ is the predicted value. All data arrangement, model development, and visualization analyses were performed using Python software (version 3.9.5).

## 3. Results and Discussion

### *3.1. Development of a Predictive Model for Dry Matter Intake Using In Vitro Volatile Fatty Acids in the Rumen*

Predicting dry matter intake (DMI) is a crucial aspect of our study, as accurate predictions can significantly reduce discrepancies between in vitro and in vivo fermentation tests. We employed various algorithms, including MLR, KNN, and ANN, to develop predictive models. Figure 1 visually represents the predicted and observed values, providing immediate insight into each model's performance.

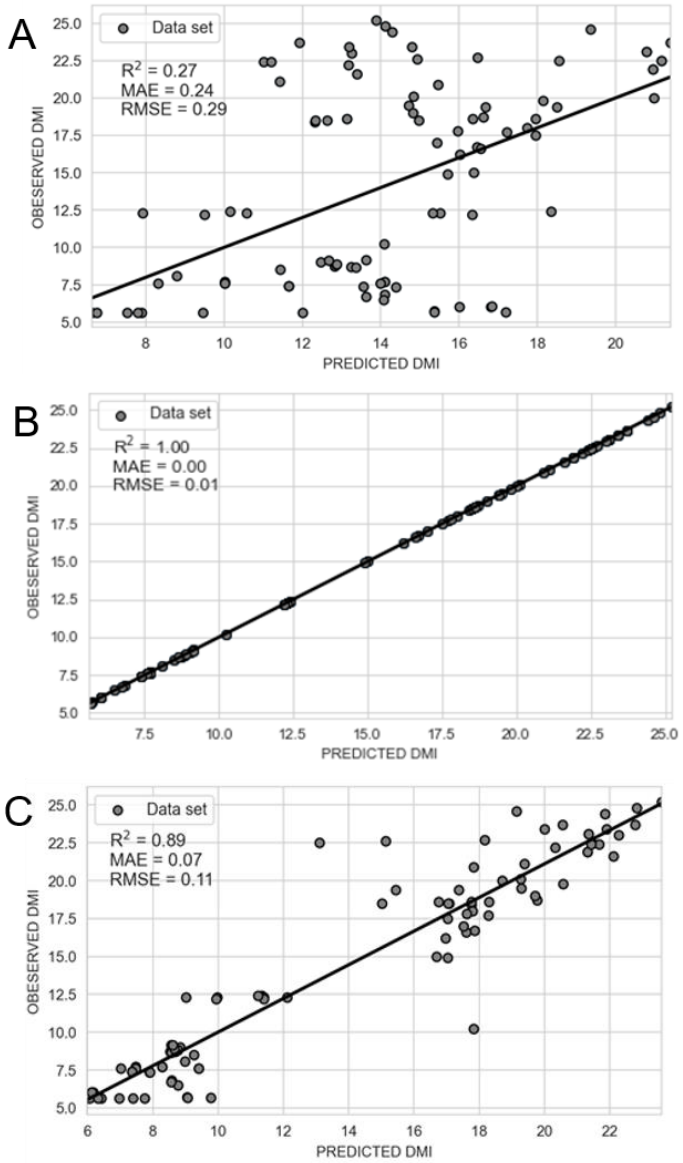



**Figure 1.** Comparison of multiple linear regression (MLR), *k*-nearest neighbor (KNN), and artificial neural network (ANN) models: (**A**) Multiple linear regression (MLR) model; (**B**) *k*-nearest neighbor (KNN) model (*k* = 1); (**C**) Artificial neural network (ANN) model; $R^2$, coefficient of determination; MAE, mean absolute error; RMSE, root mean squared error.

The observed DMI ranged from 5 to 25 kg/d. To assess model effectiveness, we used metrics such as $R^2$, MAE, and RMSE. Although these metrics do not provide absolute evaluation standards, they are essential for comparing models and identifying those with the highest predictive accuracy [61]. In Figure 1A, the MLR model shows the highest variance among the algorithms. In Figure 1B, the KNN model displays the highest predictive

accuracy, though it risks overfitting, especially with smaller values of *k* [62]. To mitigate this risk, we conducted a k-elbow test beforehand, enlarging the dataset and adjusting the *k* value using the elbow method for *K*-means clustering. The optimal *k* value was determined based on the within-cluster sum of squares, where the rate of decrease sharply slowed (the "elbow"), ensuring robustness and minimizing overfitting risks. Despite these precautions, the KNN model perfectly predicted both DMI and total digestible nutrient (TDN) levels, achieving an $R^2$ of 1. The ANN model, shown in Figure 1C, demonstrates moderate variance and achieved an $R^2$ of 0.89 when predicting DMI, indicating a notably high level of predictive accuracy.

### *3.2. Volatile Fatty Acid Prediction Model Using Nutrient Intake of Cattle*

The calculated feed nutrient intake, based on the predicted DMI values, adhered to the guidelines of the National Research Council [63], ensuring that all nutrient intakes remained within the normal range. In the development of an optimization model, the choice of an appropriate algorithm is critical as it must align with the characteristics of the data. Predicted nutrient intake values varied, with the error percentage ranging between 5% and 15%, depending on the algorithm employed. Table 3 provides insight into the regression coefficients and constants of the MLR model for predicting volatile fatty acids. These coefficients are fundamental in explaining the linear relationship between response and predictor variables [64], highlighting the intricate dynamics within the system. Observations revealed that MC2, closely related to the NDF content, increased proportionally to forage intake. Notably, MC2 (r = 0.80) displayed substantial regression coefficients for nutrient detergent fiber intake (NDFI), while MC3 exhibited the highest positive regression coefficient for DMI. The TVFA content was highest in DMI, with a notable correlation coefficient (r = 2.74). The positive correlation between DMI and TVFA concentrations highlights that, as feed intake increases, the production of volatile fatty acids also increases until microorganisms in ruminants reach a saturation point for fermentation and decomposition. In each predictive model, DMI and total digestible nutrient intake (TDNI) exhibited a negative correlation. For cows, high acetate production, associated with forage intake, is vital for milk production. The negative relationship observed in this study, based on the data of Korean cattle and dairy cattle, suggests that DMI and TDNI have a substantial impact on all volatile fatty acids, potentially offsetting high values in the prediction. Our comprehensive analysis confirmed the validity of regression coefficients for all variables at a significance level of 5% ($p < 0.05$). Consequently, further studies focusing on nutrient intake and volatile fatty acid production according to livestock breeds are essential for a precise understanding of these relationships.

**Table 3.** Summary of equations for each MLR model of coefficients and constants for predicting volatile fatty acids according to nutrient intake.

| Models * | $b_1$ | $b_2$ | $b_3$ | $b_4$ | $b_5$ | $b_6$ | $b_7$ | a | *p*-Value |
|---|---|---|---|---|---|---|---|---|---|
| MC2 | −2.64 | 0.19 | 0.26 | 0.97 | 0.80 | −0.19 | 1.00 | 0.54 | <0.05 |
| MC3 | 1.14 | −0.19 | −0.27 | −0.38 | −0.37 | −0.16 | −1.11 | 0.93 | <0.05 |
| MC4 | 1.57 | −0.21 | −0.07 | −0.19 | −0.12 | −0.07 | −0.30 | 0.12 | <0.05 |
| TVFA | 2.74 | −0.17 | −0.20 | −1.00 | −1.03 | 0.30 | −1.15 | 0.58 | <0.05 |

* Model equation = $b_1$DMI + $b_2$CPI + $b_3$EEI + $b_4$OMI + $b_5$NDFI + $b_6$ADFI + $b_7$TDNI + a; MC2, acetate (mol/100 mol); MC3, propionate (mol/100 mol); MC4, butyrate (mol/100 mol); TVFA, total volatile fatty acid (mmol/L); DMI, dry matter intake (kg/d); CPI, crude protein intake (kg/d); EEI, ether extract intake (kg/d); OMI, organic matter intake (kg/d); NDFI, neutral detergent fiber intake (kg/d); ADFI, acid detergent fiber intake (kg/d); TDNI, total digestible nutrient intake (kg/d).

Figure 2 illustrates the visualization of predicted and observed values of the volatile fatty acids MC2, MC3, and MC4 across each algorithm. When using the MLR prediction model, the $R^2$ for MC4 was 0.85, while the $R^2$ for MC3 was 0.76, emphasizing the model's accuracy in predicting MC3. The KNN-based volatile fatty acid prediction model, utilizing linear data, demonstrated superior accuracy over the other algorithms, achieving an $R^2$

of 1 and an MAE of 0. However, it is crucial to acknowledge the potential for overfitting, particularly with limited data sets. The KNN algorithm tends to overfit under such circumstances, leading to an overly optimistic estimate of the model's predictive power. In this study, the KNN algorithm showed a propensity to overfit due to the limited available data.

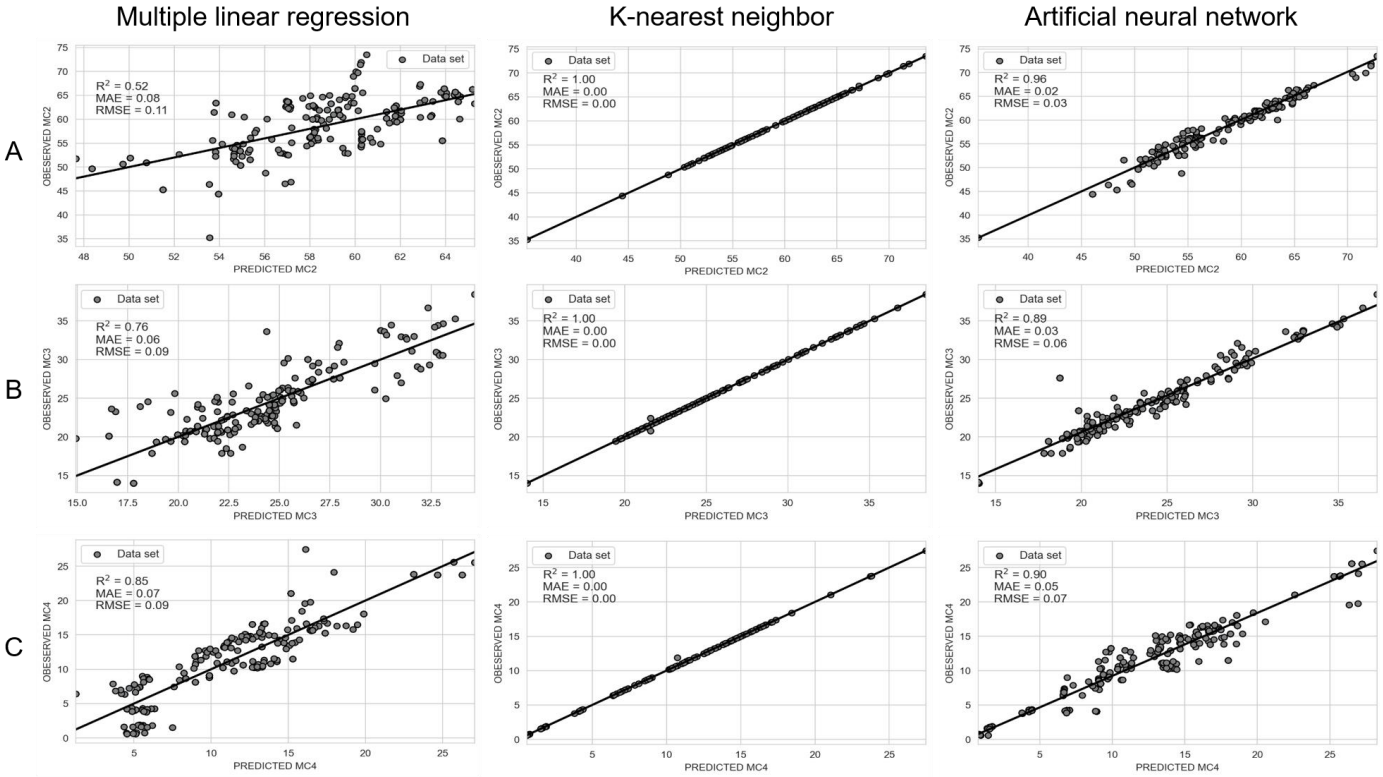



**Figure 2.** Plots of observed and predicted volatile fatty acids according to each algorithm: (**A**) Acetate (MC2, mol/100 mol); (**B**) Propionate (MC3, mol/100 mol); (**C**) Butyrate (MC4, mol/100 mol); $R^2$, coefficient of determination; MAE, mean absolute error; RMSE, root mean squared error.

The MC2 model, employing an ANN algorithm, showed exceptional performance, boasting an $R^2$ of 0.96, MAE of 0.02, and RMSE of 0.03 within a linear data distribution. Transitioning to the ANN model's predictions for MC3 and MC4 yielded $R^2$ values of 0.89 and 0.90, respectively, highlighting a high level of accuracy with the MC3 model demonstrating the greatest accuracy. The KNN model showed superior accuracy in predicting TVFA concentrations compared to the ANN and MLR models (Figure 3). Despite significant data deviation, all models demonstrated excellent performance in predicting TVFA concentrations, underscoring their robust predictive capabilities. Both KNN and ANN models emerged as the top performers among the models tested. Contrary to some studies that suggest lower accuracy when using data sets with molar ratios compared to units [65], this study demonstrates that these ratios can still provide highly accurate predictions. The overall findings underscore the robustness and reliability of the employed algorithms in predicting TVFA concentrations, even in the presence of substantial data variability.

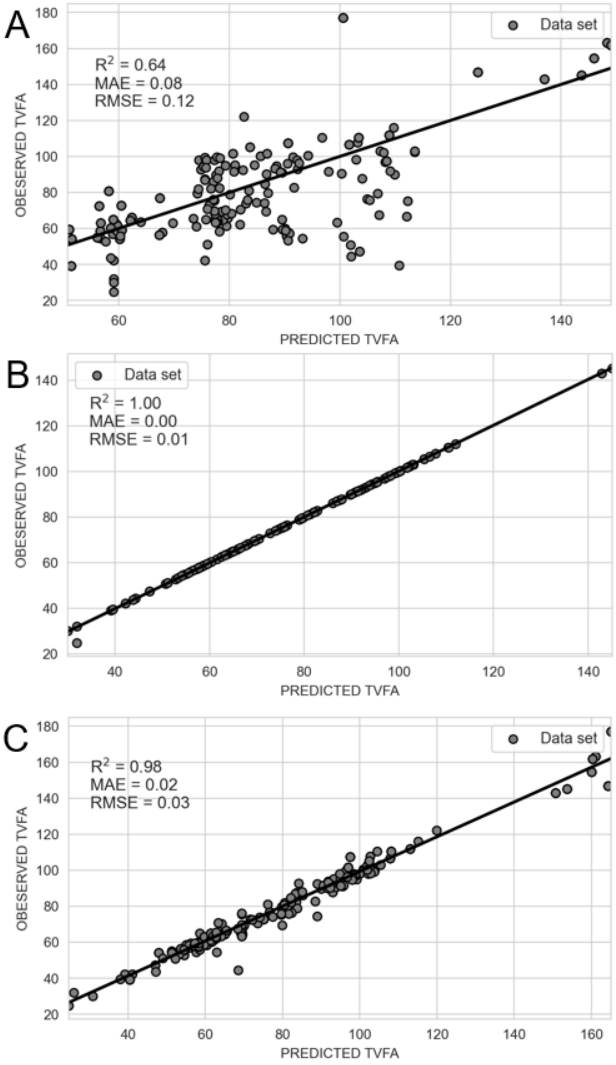



**Figure 3.** Comparison of observed and predicted values of total volatile fatty acid with the composition of nutrient intake as a dependent variable, according to each algorithm: (**A**) Multiple linear regression (MLR) model; (**B**) *k*-nearest neighbor (KNN) model ($k$ = 1); (**C**) Artificial neural network (ANN) model; $R^2$, coefficient of determination; MAE, mean absolute error; RMSE, root mean squared error.

### *3.3. Development of a Methane Prediction Model Using k Clusters of Volatile Fatty Acids*

Methanogenesis, which is intimately linked to the production of ruminal volatile fatty acids and significantly influenced by the rumen environment [66], prompted the development of a predictive model for methane production to better understand and manage its dynamics in the rumen. The resultant number of predicted data clusters with each model was three (Figure 4). Table 4 provides a summary of the methane production prediction accuracy for each algorithm and *K*-means cluster. Methanogenesis shows a high correlation with acetate considering their close association with the rumen. Furthermore, butyrate, produced during acetate–lactate fermentation, plays a role in methanogenesis [67]. Regression coefficients for MC2 and MC4 within the KM0 and KM2 clusters, as indicated in the MLR prediction equation (Table 4 footnote), highlight acetate and butyrate as critical factors in methanogenesis. A scatterplot visualizing the clustered VFAs dataset (Figure 5) allows for a comparison of the distribution of predicted methane production data with observed values.

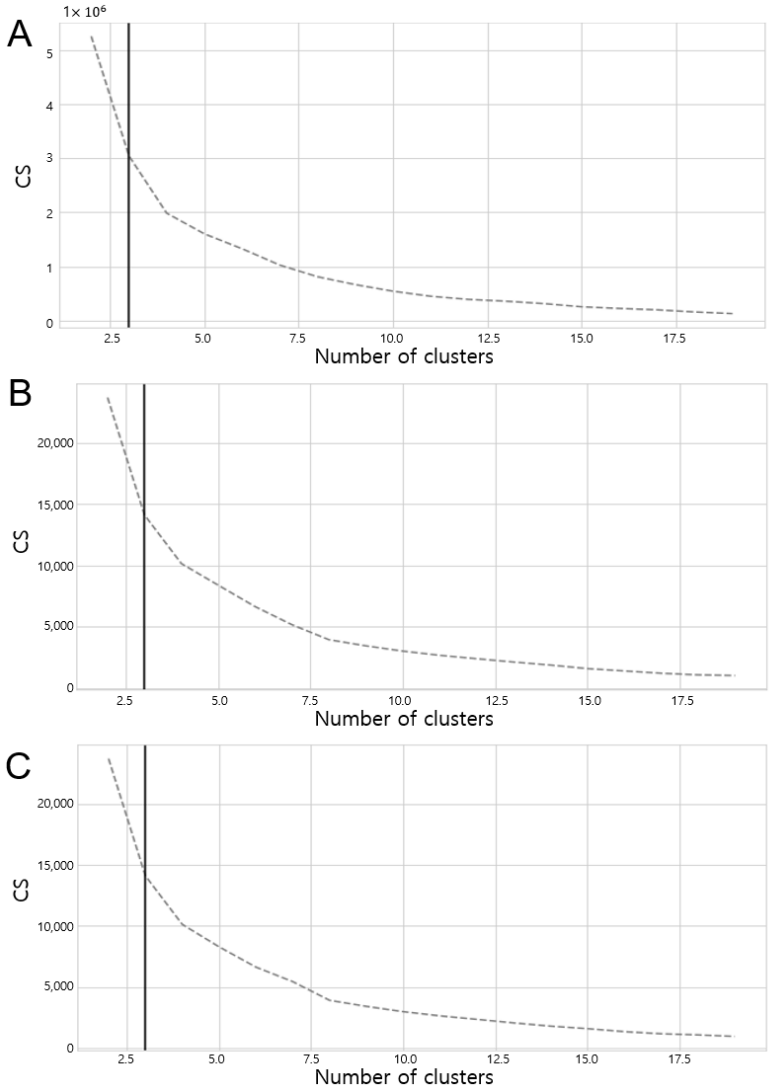



**Figure 4.** Elbow curve plot of selected *k* values for *K*-mean clusters of volatile fatty acids [68]: (**A**) Multiple linear regression (MLR) model; (**B**) *K*-nearest neighbor (KNN) model ($k$ = 1); (**C**) Artificial neural network (ANN) model; CS, within-cluster sum of squares.

In the case of MLR (Figure 5A), despite a constant slope in all clusters, the prediction accuracy was relatively low due to a wide distribution between the observed and predicted values. The KNN algorithm (Figure 5B) shows consistent prediction and observation across the clusters, except for the KM0 cluster. The deviation in the KM0 cluster may be attributed to the unique characteristics of the data, generating substantial methane despite an increase in propionate. The ANN model (Figure 5C) demonstrates a more constrained data distribution than the MLR model, except in the KM1 cluster. KNN demonstrates the lowest predictive power in the KM0 cluster, with an $R^2$ of 1 in the KM1 and KM2 clusters. For the ANN, the $R^2$ of KM1 is 0.88 and the $R^2$ of KM2 is 0.99, confirming high predictive power. MLR exhibits the lowest predictive power in KM1 and the highest error rate among the three algorithms, thereby indicating that the KNN algorithm serves as a more effective method for clustered methane prediction.

Overall, methane production varies with the production of MC2 and MC4, as butyrate, generated through acetic acid/lactic acid formation, undergoes conversion to methane along with hydrogen [9,12]. These findings confirm that the amount of methane produced by ruminants is closely linked to the concentrations of acetate and butyrate present.

**Table 4.** Comparisons of the multiple linear regression-, *k*-nearest neighbor-, and artificial neural network-based models for predicting methane production.

| Variable | | KM0 [2] | KM1 | KM2 |
|---|---|---|---|---|
| N | | 18 | 51 | 19 |
| Observed mean | | 317.88 | 313.46 | 269.46 |
| Predicted mean | | | | |
| | MLR [1] | 317.88 | 313.46 | 269.46 |
| | KNN | 327.15 | 313.46 | 269.46 |
| | ANN | 312.82 | 338.98 | 279.93 |
| $R^2$ | | | | |
| | MLR | 0.83 | 0.56 | 0.80 |
| | KNN | 0.95 | 1.00 | 1.00 |
| | ANN | 0.94 | 0.88 | 0.99 |
| MAE | | | | |
| | MLR | 0.09 | 0.16 | 0.12 |
| | KNN | 0.02 | 0.00 | 0.00 |
| | ANN | 0.05 | 0.08 | 0.03 |
| RMSE | | | | |
| | MLR | 0.11 | 0.21 | 0.14 |
| | KNN | 0.06 | 0.00 | 0.00 |
| | ANN | 0.07 | 0.11 | 0.04 |

[1] MLR, multiple linear regression; KNN, *k*-nearest neighbor; ANN, artificial neural network model; $R^2$, coefficient of determination; MAE, mean absolute error; RMSE, root mean squared error. [2] KM0 equation, 0.05MC2 − 0.96MC3 + 0.06MC4 − 0.20TVFA + 0.95 ($p < 0.05$); KM1 equation = −0.94MC2 − 0.6MC3 + 0.19MC4 + 0.16TVFA + 0.92 ($p < 0.05$); KM2 equation = 0.07MC2 − 0.48MC3 + 0.31MC4 − 0.77TVFA + 0.87 ($p < 0.05$).

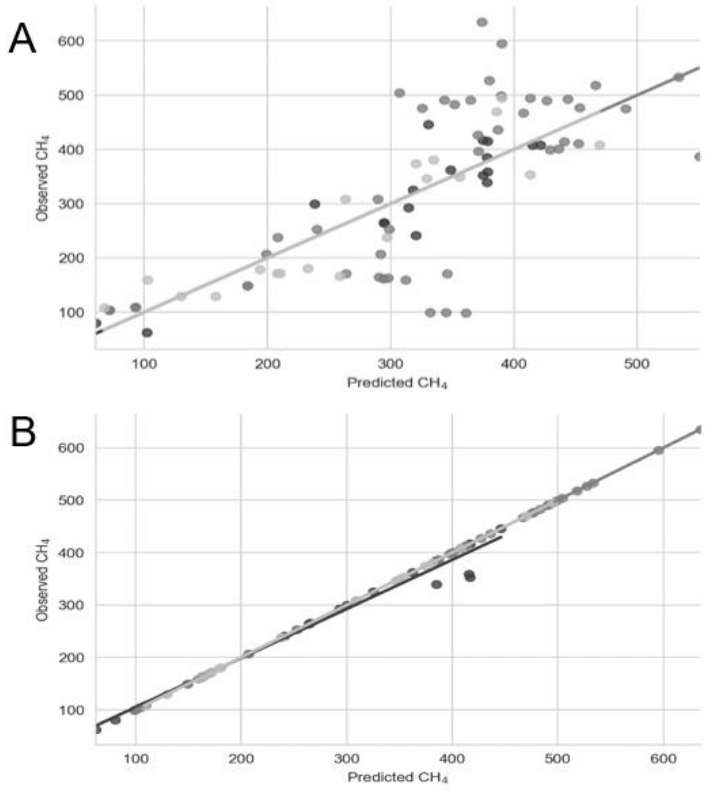



**Figure 5.** *Cont*.

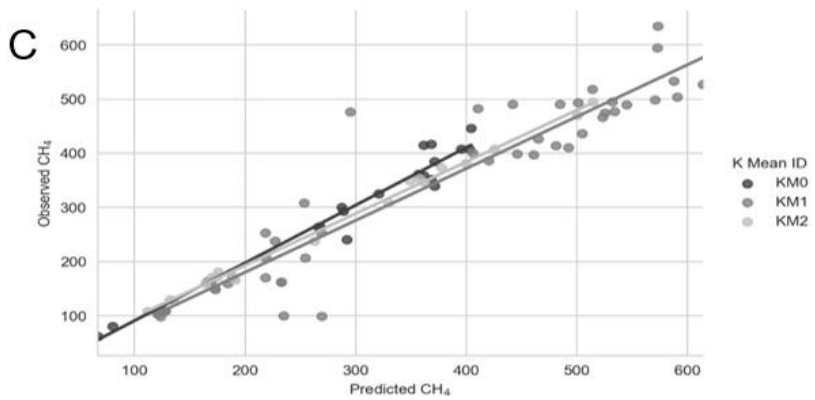



**Figure 5.** Comparison of predicted versus observed methane values cluster using the *K*-mean algorithm according to each model: (**A**) Multiple linear regression (MLR) model; (**B**) *k*-nearest neighbor (KNN) model ($k = 1$); (**C**) Artificial neural network (ANN) model; KNN model is 1 of *k* value based on the RMSE minimum.

## 4. Conclusions

This study highlights the effectiveness of employing *K*-nearest neighbor (KNN) models in predicting volatile fatty acid (VFA) concentrations from various predictors such as dry matter intake (DMI), neutral detergent fiber intake (NDFI), organic matter intake (OMI), and total digestible nutrient intake (TDN). The results demonstrate that specific VFAs, notably acetate (MC2) and butyrate (MC4), are significantly influenced by NDFI, while propionate (MC3) shows a high sensitivity to DMI. Within the *K*-means clusters used in our models (KM0, KM1, KM2), acetate and butyrate are confirmed as key factors affecting methane production. This suggests that the concentrations of these VFAs are critical in methanogenesis, as their levels significantly influence the substrates available for methanogens. The cluster analysis shows distinct patterns of influence.

The interplay among these VFAs suggests the need for tailored predictions for both VFA and methane concentrations, which may require integrating both in vitro and in vivo experimental approaches to enhance predictive accuracy. The study also underscores that increased NDFI significantly raises levels of acetate and butyrate, leading to higher methane production. This relationship indicates potential strategies to mitigate methane emissions by adjusting NDFI levels in ruminant diets, as modifying fiber intake can alter VFA production and consequently affect methanogenesis.

Measuring methane directly on farms presents significant challenges. The models we have developed for predicting volatile fatty acid (VFA) concentrations and methane emissions, validated across diverse environmental data, offer a promising solution. By utilizing dietary nutrient content and dry matter intake, these models can accurately estimate methane production. This approach provides a practical tool for both ongoing research and real-world applications in ruminant nutrition, simplifying the complex process of methane measurement and enhancing the management of dietary strategies.

When applying the model results, it is crucial to leverage the strengths and mitigate the weaknesses of each algorithm. This approach would enhance the evaluation and application of the models in predicting methane emissions and optimizing feeding strategies for ruminants. By addressing these aspects, we can refine the models' accuracy and enhance their practical utility in diverse environmental settings.

In conclusion, while our models offer valuable predictive capabilities, future research should focus on expanding the dataset to cover a broader range of conditions and conducting extensive real-world validations. By addressing these aspects, we can refine the models' accuracy and enhance their practical utility in diverse environmental settings.

**Author Contributions:** Conceptualization, S.C. and M.P.; Data curation, S.C., M.P. and E.J.; Formal analysis, N.-J.C., S.C. and M.P.; Methodology, N.-J.C., S.C. and M.P.; Software, S.C. and M.P.; Validation, N.-J.C. and E.J.; Investigation, M.P. and E.J.; Writing—original draft, M.P.; Writing—review & editing, N.-J.C., S.C., M.P. and E.J. All authors have read and agreed to the published version of the manuscript.

**Funding:** This paper was supported by research funds from Jeonbuk National University in 2024.

**Institutional Review Board Statement:** Not applicable.

**Informed Consent Statement:** Not applicable.

**Data Availability Statement:** The original contributions presented in the study are included in the article, further inquiries can be directed to the corresponding author.

**Acknowledgments:** This paper was supported by research funds of Jeonbuk National University in 2024.

**Conflicts of Interest:** The authors declare no conflict of interest.

## References

1. Siciliano-Jones, J.; Murphy, M. Production of volatile fatty acids in the rumen and cecum-colon of steers as affected by forage: Concentrate and forage physical form. *J. Dairy Sci.* **1989**, *72*, 485–492. [CrossRef] [PubMed]
2. Dijkstra, J.; Forbes, J.M.; France, J. *Quantitative Aspects of Ruminant Digestion and Metabolism*; CABI Publishing: Wallingford, UK, 2005.
3. Eom, J.-S.; Lee, S.-J.; Lee, Y.-G.; Lee, S.-S. Comparison of volatile fatty acids, monosaccharide analysis and metabolic profiling in rumen fluid according to feeding methods. *J. Korea Acad. Ind. Coop. Soc.* **2018**, *19*, 814–824. [CrossRef]
4. Grant, D.; Patel, P. Changes of protein composition of milk by ratio of roughage to concentrate. *J. Dairy Sci.* **1980**, *63*, 756–761. [CrossRef]
5. Urrutia, N.L.; Harvatine, K.J. Acetate dose-dependently stimulates milk fat synthesis in lactating dairy cows. *J. Nutr.* **2017**, *147*, 763–769. [CrossRef]
6. Church, D.C. *The Ruminant Animal: Digestive Physiology and Nutrition*; Waveland Press: Long Grove, IL, USA, 1993.
7. Ko, M.-J.; Kim, D.-S.; Jeong, S.-Y.; Kim, B.; Kang, O.-D.; Lee, S.-C.; Lee, W.-S.; Farm, N.D. The effects of sodium bicarbonate and liquid buffer on milk yield, milk composition and blood metabolites of Holstein dairy cows. *J. Agric. Life Sci.* **2014**, *48*, 243–251. [CrossRef]
8. Sander, E.; Warner, R.; Harrison, H.; Loosli, J. The stimulatory effect of sodium butyrate and sodium propionate on the development of rumen mucosa in the young calf. *J. Dairy Sci.* **1959**, *42*, 1600–1605. [CrossRef]
9. Ha, J.; Lee, S.; Moon, Y.; Kim, C.; Seo, S.; Beak, M.; Lee, S.; Lee, S.; Lee, W.; Jang, J. *Ruminant Nutrition and Physiology*; Seoul National University Press: Seoul, Republic of Korea, 2005.
10. Grobner, M.; Johnson, D.; Goodall, S.; Benz, D. Sarsaponin Effects on in vitro Continuous Flow Fermentation of a High Grain Diet. In Proceedings of the Annual Meeting, New York, NY, USA, 28–30 December 1982; American Society for Animal Science Western Section: Champaign, IL, USA, 1982.
11. Jouany, J.-P.; Morgavi, D. Use of 'natural' products as alternatives to antibiotic feed additives in ruminant production. *Animal* **2007**, *1*, 1443–1466. [CrossRef] [PubMed]
12. Kim, J.; Yoon, Y.-M.; Kim, C.-H. Effects of supplementation of mixed methanogens and rumen cellulolytic bacteria on biochemical Methane potential. *Korean J. Soil Sci. Fertil.* **2012**, *45*, 515–523. [CrossRef]
13. Johnson, K.A.; Johnson, D.E. Methane emissions from cattle. *J. Anim. Sci.* **1995**, *73*, 2483–2492. [CrossRef]
14. Field, C.B.; Barros, V.R. *Climate Change 2014–Impacts, Adaptation and Vulnerability: Regional Aspects*; Cambridge University Press: Cambridge, UK, 2014.
15. Sveinbjörnsson, J.; Huhtanen, P.; Udén, P. The Nordic dairy cow model, Karoline-development of volatile fatty acid sub-model. In *Nutrient Digestion and Utilization in Farm Animals: Modelling Approaches*; CABI Publishing: Wallingford UK, 2006; pp. 1–14.
16. Bannink, A.; Kogut, J.; Dijkstra, J.; France, J.; Kebreab, E.; Van Vuuren, A.; Tamminga, S. Estimation of the stoichiometry of volatile fatty acid production in the rumen of lactating cows. *J. Theor. Biol.* **2006**, *238*, 36–51. [CrossRef]
17. Morvay, Y.; Bannink, A.; France, J.; Kebreab, E.; Dijkstra, J. Evaluation of models to predict the stoichiometry of volatile fatty acid profiles in rumen fluid of lactating Holstein cows. *J. Dairy Sci.* **2011**, *94*, 3063–3080. [CrossRef]
18. Robinson, D.L.; Goopy, J.; Hegarty, R. Can rumen Methane production be predicted from volatile fatty acid concentrations? *Anim. Prod. Sci.* **2010**, *50*, 630–636. [CrossRef]
19. Jayanegara, A.; Ikhsan, I.; Toharmat, T. Assessment of Methane estimation from volatile fatty acid stoichiometry in the rumen in vitro. *J. Indones. Trop. Anim. Agric.* **2013**, *38*, 103–108. [CrossRef]
20. Williams, S.R.O.; Hannah, M.C.; Jacobs, J.L.; Wales, W.J.; Moate, P.J. Volatile fatty acids in ruminal fluid can be used to predict Methane yield of dairy cows. *Animals* **2019**, *9*, 1006. [CrossRef] [PubMed]

21. van Lingen, H.J.; Fadel, J.G.; Moraes, L.E.; Bannink, A.; Dijkstra, J. Bayesian mechanistic modeling of thermodynamically controlled volatile fatty acid, hydrogen and Methane production in the bovine rumen. *J. Theor. Biol.* **2019**, *480*, 150–165. [CrossRef] [PubMed]
22. Craninx, M.; Fievez, V.; Vlaeminck, B.; De Baets, B. Artificial neural network models of the rumen fermentation pattern in dairy cattle. *Comput. Electron. Agric.* **2008**, *60*, 226–238. [CrossRef]
23. Zhao, Y.; Morgan, M.A.; Sun, Y. Targeting Neddylation pathways to inactivate cullin-RING ligases for anticancer therapy. *Antioxid. Redox Signal.* **2014**, *21*, 2383–2400. [CrossRef] [PubMed]
24. Li, M.M.; Sengupta, S.; Hanigan, M.D. Using artificial neural networks to predict pH, ammonia, and volatile fatty acid concentrations in the rumen. *J. Dairy Sci.* **2019**, *102*, 8850–8861. [CrossRef] [PubMed]
25. Song, Y.; Liang, J.; Lu, J.; Zhao, X. An efficient instance selection algorithm for k nearest neighbor regression. *Neurocomputing* **2017**, *251*, 26–34. [CrossRef]
26. Ahn, J.-S.; Shin, J.-S.; Chung, K.-Y.; Lim, H.; Choi, J.-G.; Kim, J.-H.; Kwon, E.-G.; Park, B.-K. Changes in ruminal fermentable characteristics and nutrient degradabilities of corn flake according to chamber type in Hanwoo: Chamber type for corn flake in the rumen of Hanwoo. *Korean J. Agric. Sci.* **2018**, *45*, 695–706. [CrossRef]
27. Beauchemin, K.; McGinn, S. Methane emissions from feedlot cattle fed barley or corn diets. *J. Anim. Sci.* **2005**, *83*, 653–661. [CrossRef] [PubMed]
28. Beauchemin, K.; McGinn, S. Methane emissions from beef cattle: Effects of fumaric acid, essential oil, and canola oil. *J. Anim. Sci.* **2006**, *84*, 1489–1496. [CrossRef]
29. Beauchemin, K.; McGinn, S.; Martinez, T.; McAllister, T. Use of condensed tannin extract from quebracho trees to reduce Methane emissions from cattle. *J. Anim. Sci.* **2007**, *85*, 1990–1996. [CrossRef]
30. Beauchemin, K.; McGinn, S.; Benchaar, C.; Holtshausen, L. Crushed sunflower, flax, or canola seeds in lactating dairy cow diets: Effects on Methane production, rumen fermentation, and milk production. *J. Dairy Sci.* **2009**, *92*, 2118–2127. [CrossRef]
31. Benchaar, C.; Hassanat, F.; Gervais, R.; Chouinard, P.; Julien, C.; Petit, H.; Massé, D. Effects of increasing amounts of corn dried distillers grains with solubles in dairy cow diets on Methane production, ruminal fermentation, digestion, N balance, and milk production. *J. Dairy Sci.* **2013**, *96*, 2413–2427. [CrossRef] [PubMed]
32. Biswas, A.A.; Lee, S.S.; Mamuad, L.L.; Kim, S.H.; Choi, Y.J.; Lee, C.; Lee, K.; Bae, G.S.; Lee, S.S. Effects of illite supplementation on in vitro and in vivo rumen fermentation, microbial population and Methane emission of Hanwoo steers fed high concentrate diets. *Anim. Sci. J.* **2018**, *89*, 114–121. [CrossRef]
33. Bougouin, A.; Ferlay, A.; Doreau, M.; Martin, C. Effects of carbohydrate type or bicarbonate addition to grass silage-based diets on enteric Methane emissions and milk fatty acid composition in dairy cows. *J. Dairy Sci.* **2018**, *101*, 6085–6097. [CrossRef] [PubMed]
34. Bougouin, A.; Martin, C.; Doreau, M.; Ferlay, A. Effects of starch-rich or lipid-supplemented diets that induce milk fat depression on rumen biohydrogenation of fatty acids and methanogenesis in lactating dairy cows. *Animal* **2019**, *13*, 1421–1431. [CrossRef]
35. Guyader, J.; Eugène, M.; Meunier, B.; Doreau, M.; Morgavi, D.; Silberberg, M.; Rochette, Y.; Gerard, C.; Loncke, C.; Martin, C. Additive Methane-mitigating effect between linseed oil and nitrate fed to cattle. *J. Anim. Sci.* **2015**, *93*, 3564–3577. [CrossRef]
36. Hassanat, F.; Gervais, R.; Massé, D.; Petit, H.; Benchaar, C. Methane production, nutrient digestion, ruminal fermentation, N balance, and milk production of cows fed timothy silage-or alfalfa silage-based diets. *J. Dairy Sci.* **2014**, *97*, 6463–6474. [CrossRef]
37. Hatew, B.; Podesta, S.; Van Laar, H.; Pellikaan, W.; Ellis, J.; Dijkstra, J.; Bannink, A. Effects of dietary starch content and rate of fermentation on Methane production in lactating dairy cows. *J. Dairy Sci.* **2015**, *98*, 486–499. [CrossRef] [PubMed]
38. Holtshausen, L.; Chaves, A.; Beauchemin, K.; McGinn, S.; McAllister, T.; Odongo, N.; Cheeke, P.; Benchaar, C. Feeding saponin-containing *Yucca schidigera* and *Quillaja saponaria* to decrease enteric Methane production in dairy cows. *J. Dairy Sci.* **2009**, *92*, 2809–2821. [CrossRef]
39. Jeon, S.; Jeong, S.; Lee, M.; Seo, J.; Kam, D.K.; Kim, J.H.; Park, J.; Seo, S. Effects of reducing inclusion rate of roughages by changing roughage sources and concentrate types on intake, growth, rumen fermentation characteristics, and blood parameters of Hanwoo growing cattle (*Bos Taurus coreanae*). *Asian-Australas. J. Anim. Sci.* **2019**, *32*, 1705–1714. [CrossRef] [PubMed]
40. Jeong, C.-D.; Mamuad, L.L.; Ko, J.Y.; Sung, H.G.; Park, K.K.; Lee, Y.K.; Lee, S.-S. Rumen fermentation and performance of Hanwoo steers fed total mixed ration with Korean rice wine residue. *J. Anim. Sci. Technol.* **2016**, *58*, 4. [CrossRef]
41. Kim, S.; Alam, M.; Gu, M.; Park, K.; Jeon, C.O.; Ha, J.K.; Cho, K.; Lee, S. Effect of total mixed ration with fermented feed on ruminal in vitro fermentation, growth performance and blood characteristics of Hanwoo steers. *Asian-Australas. J. Anim. Sci.* **2012**, *25*, 213. [CrossRef] [PubMed]
42. Kim, H.; Lee, S.; Jeong, S.; Park, J.; Shin, T.; Cho, B.; Cho, S.; Kim, B.; Seo, J. Nutrient analysis and in vitro rumen fermentation of commercial formulated concentrates for finishing Hanwoo steers. *Korean J. Agric. Sci.* **2016**, *43*, 802–809. [CrossRef]
43. Kim, D.H.; Park, H.Y.; Choi, C.W. Comparison of in vitro ruminal fermentation between different originated corn grains. *Korean J. Agric. Sci.* **2017**, *44*, 541–548. [CrossRef]
44. Kim, S.H.; Ramos, S.C.; Jeong, C.D.; Mamuad, L.L.; Park, K.K.; Cho, Y.I.; Son, A.; Lee, S.-S. Growth performance and blood profiles of Hanwoo steers at fattening stage fed Korean rice wine residue. *J. Anim. Sci. Technol.* **2020**, *62*, 812–823. [CrossRef]
45. Kook, K.; Chung, W.-T.; Park, H.-S.; Jang, K.-Y.; Lee, J.-W.; Moon, S.-J.; Kim, K.-H. The Effects of Aqueous Fibrolytic Enzyme Products Supplementation on In vitro Fermentation and Growth Performance of Hanwoo Steers. *J. Anim. Sci. Technol.* **2009**, *51*, 39–44. [CrossRef]

46. Lee, A.; Shin, S.-J.; Yang, J.; Cho, S.; Choi, N.-J. Effect of lactic acid bacteria and enzyme supplementation on fermentative patterns of ensiling silages, their in vitro ruminal fermentation, and digestibility. *J. Korean Soc. Grassl. Forage Sci.* **2016**, *36*, 7–14. [CrossRef]
47. Lee, H.S.; Lee, S.D.; Lee, S.; Sun, S.; Kim, M.; Choi, H.; Lee, Y.; Baek, Y.-C. Comparative evaluation of nutritional values in different forage sources using in vitro and in vivo rumen fermentation in Hanwoo cattle. *Korean J. Agric. Sci.* **2020**, *47*, 941–949. [CrossRef]
48. Mamuad, L.L.; Kim, S.H.; Ku, M.J.; Lee, S.S. Effect of γ-aminobutyric acid producing bacteria on in vitro rumen fermentation, growth performance, and meat quality of Hanwoo steers. *Asian-Australas. J. Anim. Sci.* **2020**, *33*, 1087–1095. [CrossRef]
49. Miguel, M.; Mamuad, L.; Ramos, S.; Ku, M.J.; Jeong, C.D.; Kim, S.H.; Cho, Y.I.; Lee, S.S. Effects of using different roughages in the total mixed ration inoculated with or without coculture of *Lactobacillus acidophilus* and *Bacillus subtilis* on in vitro rumen fermentation and microbial population. *Anim. Biosci.* **2021**, *34*, 642–651. [CrossRef] [PubMed]
50. Moate, P.; Williams, S.; Jacobs, J.; Hannah, M.; Beauchemin, K.; Eckard, R.; Wales, W. Wheat is more potent than corn or barley for dietary mitigation of enteric Methane emissions from dairy cows. *J. Dairy Sci.* **2017**, *100*, 7139–7153. [CrossRef] [PubMed]
51. Nogoy, K.M.C.; Yu, J.; Song, Y.G.; Li, S.; Chung, J.-W.; Choi, S.H. Evaluation of the Nutrient Composition, In Vitro Fermentation Characteristics, and In Situ Degradability of *Amaranthus caudatus*, *Amaranthus cruentus*, and *Amaranthus hypochondriacus* in Cattle. *Animals* **2021**, *11*, 18. [CrossRef] [PubMed]
52. Park, S.H.; Baek, Y.C.; Lee, S.; Kim, B.H.; Ryu, C.H. Evaluation the Feed Value of Whole Crop Rice Silage and Comparison of Rumen Fermentation according to Its Ratio. *J. Korean Soc. Grassl. Forage Sci.* **2020**, *40*, 236–243. [CrossRef]
53. Van Zijderveld, S.; Fonken, B.; Dijkstra, J.; Gerrits, W.; Perdok, H.; Fokkink, W.; Newbold, J. Effects of a combination of feed additives on Methane production, diet digestibility, and animal performance in lactating dairy cows. *J. Dairy Sci.* **2011**, *94*, 1445–1454. [CrossRef] [PubMed]
54. Yang, S.-J.; Jung, E.-S.; Kim, H.-B.; Shin, T.-S.; Cho, B.-W.; Cho, S.-K.; Kim, B.-W.; Seo, J.-K. Nutritional evaluation of rice with different processing treatments on in vitro rumen fermentation characteristics and in situ degradation. *Korean J. Org. Agric.* **2018**, *26*, 281–296. [CrossRef]
55. Yang, S.J.; Kim, H.B.; Moon, J.B.; Kim, N.E.; Park, J.K.; Park, B.K.; Lee, S.Y.; Seo, J. Nutritional evaluation of total mixed rations containing rice grain in an in vitro rumen fermentation system. *Korean J. Agric. Sci.* **2018**, *45*, 741–748. [CrossRef]
56. Yoo, D.-K.; Moon, J.-B.; Kim, H.-B.; Yang, S.-J.; Park, J.-K.; Lee, S.-Y.; Seo, J.-K. Rumen Fermentation was Changed by Feed Inoculation Method in In Vitro. *Ann. Anim. Resour. Sci.* **2019**, *30*, 111–120. [CrossRef]
57. McDougall, E. The composition and output of sheep's saliva. *Biochem. J.* **1948**, *43*, 99–109. [CrossRef] [PubMed]
58. Lopez, S.; Valdes, C.; Newbold, C.; Wallace, R. Influence of sodium fumarate addition on rumen fermentation in vitro. *Br. J. Nutr.* **1999**, *81*, 59–64. [CrossRef] [PubMed]
59. Erwin, E.; Marco, G.J.; Emery, E. Volatile fatty acid analyses of blood and rumen fluid by gas chromatography. *J. Dairy Sci.* **1961**, *44*, 1768–1771. [CrossRef]
60. Chaney, A.L.; Marbach, E.P. Modified reagents for determination of urea and ammonia. *Clin. Chem.* **1962**, *8*, 130–132. [CrossRef] [PubMed]
61. Jin, C.; Lee, G. Spatial hedonic modeling using geographically weighted LASSO model. *J. Korean Geogr. Soc.* **2014**, *49*, 917–934.
62. Chu, J.; Liu, X.; Zhang, Z.; Zhang, Y.; He, M. A novel method overcomeing overfitting of artificial neural network for accurate prediction: Application on thermophysical property of natural gas. *Case Stud. Therm. Eng.* **2021**, *28*, 101406. [CrossRef]
63. Council, N.R. *Nutrient Requirements of Dairy Cattle: 2001*; National Academies Press: Washington, DC, USA, 2001.
64. Um, Y. Testing the Equality of Two Linear Regression Models: Comparison between Chow Test and a Permutation Test. *J. Korea Soc. Comput. Inf.* **2021**, *26*, 157–164. [CrossRef]
65. Bannink, A.; De Visser, H.; Klop, A.; Dijkstra, J.; France, J. Causes of Inacurate Prediction of Volatile Fatty Acids by Simulation Models of Rumen Function in Lactating Cows. *J. Theor. Biol.* **1997**, *189*, 353–366. [CrossRef]
66. Schären, M.; Seyfang, G.; Steingass, H.; Dieho, K.; Dijkstra, J.; Hüther, L.; Frahm, J.; Beineke, A.; von Soosten, D.; Meyer, U. The effects of a ration change from a total mixed ration to pasture on rumen fermentation, volatile fatty acid absorption characteristics, and morphology of dairy cows. *J. Dairy Sci.* **2016**, *99*, 3549–3565. [CrossRef]
67. Jonker, A.; Hickey, S.; Boma, P.; Woju, C.W.; Sandoval, E.; MacLean, S.; Calzada, M.G.R.; Yu, W.; Lewis, S.; Janssen, P.H. Individual-level correlations of rumen volatile fatty acids with enteric Methane emissions for ranking Methane yield in sheep fed fresh pasture. *Anim. Prod. Sci.* **2020**, *61*, 300–305. [CrossRef]
68. Kodinariya, T.M.; Makwana, P.R. Review on determining number of Cluster in *K*-Means Clustering. *Int. J.* **2013**, *1*, 90–95.


**Disclaimer/Publisher's Note:** The statements, opinions and data contained in all publications are solely those of the individual author(s) and contributor(s) and not of MDPI and/or the editor(s). MDPI and/or the editor(s) disclaim responsibility for any injury to people or property resulting from any ideas, methods, instructions or products referred to in the content.